

Giant edge spin accumulation in a symmetric quantum well with two subbands

Alexander Khaetskii¹ and J. Carlos Egues²

¹*Department of Physics, University at Buffalo, SUNY, Buffalo, NY 14260-1500*

²*Instituto de Física de São Carlos, Universidade de São Paulo, 13560-970, São Carlos, São Paulo, Brazil*

(Dated: June 14, 2018)

We have studied the edge spin accumulation due to an electric current in a high mobility two-dimensional electron gas formed in a symmetric well with two subbands. This study is strongly motivated by the recent experiment of Hernandez *et al.* [Phys. Rev. B **88**, 161305(R) (2013)] who demonstrated the spin accumulation near the edges of a symmetric bilayer GaAs structure in contrast to no effect in a single-layer configuration. The intrinsic mechanism of the spin-orbit (SO) interaction we consider arises from the coupling between two subband states of opposite parities. We obtain a parametrically large magnitude of the edge spin density for a two-subband well as compared to the usual single-subband structure. We show that the presence of a gap in the system, i.e., the energy separation Δ between the two subband bottoms, changes drastically the picture of the edge spin accumulation. The gap value governs the effective strength of the inter-subband SO interaction which provides a controllable crossover from the regime of weak spin accumulation to the regime of strong one by varying the Fermi energy (electron density) and/or Δ . We estimate that by changing the gap Δ from zero up to $1 \div 2$ K, the magnitude of the effect changes by three orders of magnitude. This opens up the possibility for the design of new spintronic devices.

PACS numbers: 72.25.-b, 73.23.-b, 73.50.Bk

Spin current and spin accumulation [1, 2] which appear due to the spin-orbit (SO) coupling in the presence of electric currents are topics of great current interest which are important for the future of spin electronics [3]. There are two distinct SO mechanisms, the extrinsic one due to the Mott asymmetry in the electron scattering off impurities [4–7], and the intrinsic one [8, 9] due to SO induced splitting of the electron spectrum. The edge spin-density accumulation, related to either the Mott asymmetry by impurities [10] (2D electrons) or the intrinsic mechanism (2D holes) [11, 12], has been experimentally observed.

It is known [2, 13–15] that in the diffusive regime (and when the spin diffusion length is much larger than the mean free path) the edge spin density is entirely due to the spin flux coming from the bulk. In contrast, the physics of the edge spin-density accumulation for the intrinsic mechanism in the opposite case of strong SO splitting [16] only recently has been understood [17–21]. This includes the experimentally important case of a diffusive sample with a large SO splitting of the spectrum so that the spin-precession length is smaller than the mean free path. This we term the quasi-ballistic regime [20,21]. In particular, for 2D holes in this regime the edge spin-density, which is due to the spin current from the bulk, is parametrically smaller than the density generated upon the boundary scattering [21].

Recently, using Kerr rotation spectroscopy, Hernandez *et al.* [22] demonstrated electric-current induced spin accumulation near the edges of a high-mobility two-dimensional electron gas in a *symmetric* bilayer GaAs structure in contrast to *no accumulation* in a single-layer configuration [23]. This result is interesting and intriguing in many aspects. The observed effect is quite large despite the fact that the electric field in the high-mobility

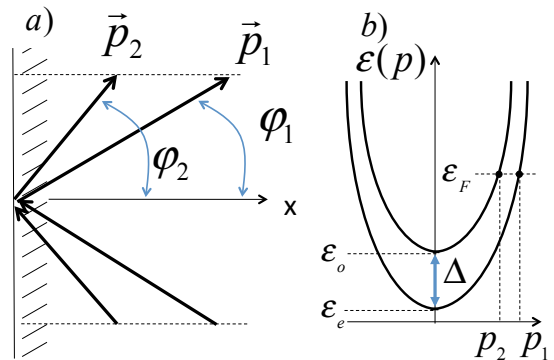


Figure 1. Schematics of the boundary specular scattering in the presence of SO coupling. Plus and minus modes are shown for the same energy and the same wave vectors along the boundary.

channel is $300 \div 400$ times smaller than that in the experiment by Kato *et al.* [10], where for a GaAs sample the result was explained by the extrinsic interaction with impurities. Note that the structure studied in [22] has inversion symmetry and therefore the usual Rashba term [24] is absent. On the other hand, the linear-in-momentum term [25] originating from a cubic Dresselhaus term is known not to lead to a spin current in the bulk. A significant difference between the observed edge spin density in the two-subband vs. the one-subband cases has motivated us to look for the explanation of this phenomenon using the inter-subband Rashba-like Hamiltonian arising in two-subband wells [26],[27].

Here we follow the method proposed in [21] to calcu-

late the edge spin density which appears due to boundary scattering [Fig. 1(a)] in the quasi-ballistic regime for a Rashba-like Hamiltonian [26],[27] describing the two-subband well [Fig. 1(b)]. In this quasi-ballistic regime the characteristic length of the spin accumulation near the boundary is smaller than the mean free path. Since the latter is around $30 \mu m$ [22], it indeed exceeds all the characteristic lengths of our theory. We have explained the experimental results, in particular, the large magnitude of the edge spin density for the two-subband sample compared to the usual single-band structure with either the Rashba or Dresselhaus interactions.

Two bands vs one band case. Interestingly, we have found that despite the problem in question resembling very much the usual Rashba problem (there are two copies of them because each state is doubly degenerate), the presence of the gap Δ between two sub-band edges [Fig. 1(b)] changes the physics of the edge spin accumulation completely. This happens because the gap magnitude governs the effective strength of the inter-subband SO interaction leading to different solutions compared to the one-band Rashba case for the occupation numbers of the incoming states participating in the boundary scattering, [Fig. 1(a)].

The physics is now determined by the value of the parameter $\xi = 2\eta k_F/\Delta \equiv L_\Delta/L_s$ [Fig. 2a], where $L_\Delta = \hbar v_F/\Delta$, $L_s = \hbar^2/2m\eta$ are the coherence and the spin-precession lengths. Here $p_F = \hbar k_F = mv_F$ is the Fermi momentum, η is the inter-subband SO coupling constant [26, 27]. The parameter ξ can have an arbitrary value even for a small η since the gap Δ can be made much smaller than the Fermi energy.

First of all, the presence of the gap changes the "helicity" direction which corresponds to the eigenvectors of the Hamiltonian (2), see Eqs. (S2), (S3) in the Supplemental Material (SM). For the two sub-band problem the helicity axis for a given momentum p is defined by the angle $\theta(p)$ with the z -axis (the normal to the 2D plane), $\cos\theta = 1/\sqrt{1+(2\eta p/\hbar\Delta)^2}$. When Δ is much bigger than the SO energy $2\eta p/\hbar$, then the helicity axis coincides with the z -axis. In the opposite case when $\Delta \rightarrow 0$ and the SO energy dominates, the helicity axis lies within the $x-y$ plane, as it should be for usual Rashba model (which corresponds to $\theta \rightarrow \pi/2$). Therefore, $\sin\theta = (2\eta p/\hbar)/\sqrt{(2\eta p/\hbar)^2 + \Delta^2}$ determines the *effective* strength of SO coupling, and the usual Rashba single-band model (in our case we have two copies of them) corresponds to a limit of strong SO coupling ($\sin\theta = 1$).

As it has been shown in [20, 21] [see also Eq. (7) below], because of the unitarity of the boundary scattering the magnitude of the edge spin accumulation is proportional to the difference $f_1(\varepsilon_F, k_y) - f_2(\varepsilon_F, k_y)$ between the distribution functions of the incoming electron states belonging to the sub-bands 1 and 2 for a given Fermi energy and given wave vector k_y along the boundary, see Fig. 1. (In the case of one-band Rashba model the incom-

ing states belong to the branches of opposite helicities). These distribution functions are found from the solution of the kinetic equation for the spin-density matrix in the bulk (2D) of the sample in the presence of impurity scattering and an electric field [28], [29] and used as the input parameters for the boundary scattering problem.

The important point is that in the one-band Rashba case the difference of the distribution functions in question is of the third order with respect to $p_1 - p_2 = \hbar/L_s$ for any reasonably short-ranged impurity potential in the bulk (when the correlation radius of the impurity potential d is much smaller than L_s). This has been rigorously proven in Ref. [21] (see Eqs. (14-16) in [21]). Thus, in the leading order (i.e. $\propto 1/L_s$) the above mentioned distribution functions take the form which they have in the absence of any spin-orbit coupling. The first order effect appears only for very smooth impurity potential when $d > L_s$, and the magnitude of the edge spin density for the one-band Rashba case is given by the expressions [21]

$$\langle S_z \rangle \simeq \frac{k_E}{L_s} \frac{d^2}{L_s^2} \text{ at } d \ll L_s; \quad \langle S_z \rangle \simeq \frac{k_E}{L_s} \text{ at } d > L_s. \quad (1)$$

Here $k_E = eE\tau_{tr}/\hbar$, e is the modulus of the electron charge, E is the magnitude of the in-plane (driving) electric field directed along the y -axis and τ_{tr} is the transport scattering time due to the impurities in the bulk of a sample. Note that we consider in our paper the case $d \ll L_s$, which is only the realistic one.

Note that the cancellation of the effect for the Rashba model in the leading order (i.e. $\propto 1/L_s$) happens when the transition rates between branches of opposite helicities have the same strength as the transition rates within the branch of the same helicity (one of the necessary conditions). That is why for smooth impurity potential ($d > L_s$) which cannot support the transitions between branches of opposite helicities, one observes the recovering of the first order effect, see Eq. (1).

From the above considerations we can immediately understand the role of the gap Δ in the two-subband model considered in this work. As explained above, the effective SO interaction decreases with increasing Δ . This causes suppression of the inter-subband transition rates, since these transitions are accompanied by spin flip, as compared to the intra-subband ones, which do not need spin flip. The suppression factor is $\sin^2\theta$, which is the probability of spin-flip (see also SM, Sec. III). Since the inter-band and intra-band rates are different now, this prevents the complete cancellation that occurs for the quantity $f_1(\varepsilon_F, k_y) - f_2(\varepsilon_F, k_y)$ in the one-band Rashba model, and leads to the recovery of the first order effect with respect to small splitting $p_1 - p_2 \ll p_F$ even for a short-ranged ($d \ll L_s$) impurity potential.

As we discuss later on, for a GaAs structure similar to that used in Ref. [22], it is enough to change the gap Δ from zero up to about $1 \div 2$ K in order to increase the magnitude of the effect by the three orders ("giant effect").

The most pronounced change happens at $L_\Delta \simeq 0.5L_s$, where the edge spin density $S_z(x)$ is maximized and its order of magnitude is given by k_E/L_s , which is parametrically larger than in the single-band case [Fig. 2a].

We consider specular scattering [i.e., a straight boundary for simplicity, Fig. 1(a)] and a Fermi energy much larger than the gap Δ between the subbands, i.e., $\varepsilon_F \gg \Delta$ [30]. Moreover, the SO interaction is weak ($\eta k_F \ll \varepsilon_F$) and therefore "coherent" and spin-precession length scales are large compared to the Fermi wave length, $L_\Delta, L_s \gg \lambda_F = 2\pi/k_F$. The ratio L_Δ/L_s can be arbitrary. Our calculation shows that the characteristic spatial scale of the edge spin density is $\Lambda = L_\Delta L_s / \sqrt{L_\Delta^2 + L_s^2}$.

Model Hamiltonian. The Hamiltonian of a symmetric quantum well with two subbands and inter-subband-induced SO interaction resembles that of the ordinary Rashba model. In contrast to the latter, the intersubband SO interaction is nonzero even in symmetric structures with the 4×4 Hamiltonian is [26], [27]

$$H = \left(\frac{p^2}{2m} + \varepsilon_+\right)1 \otimes 1 - \varepsilon_- \tau_z \otimes 1 + \left(\frac{\eta}{\hbar}\right)\tau_x \otimes (p_x \sigma_y - p_y \sigma_x) \quad (2)$$

Here \otimes means a direct tensor product, m is the effective mass, $\varepsilon_\pm = (\varepsilon_o \pm \varepsilon_e)/2$, ε_e and ε_o are quantized energies of the lowest (even) and first excited (odd) subbands, respectively, measured from the bottom of the quantum well, $\tau_{x,y,z}$ denote the Pauli matrices describing the sub-band (or pseudospin) degree of freedom, and $\sigma_{x,y,z}$ are Pauli matrices referring to the electron spin. The inter-subband SO coupling η (which has the dimensionality of square of charge) is expressed [26] in terms of the gradients of the Hartree-type contribution to the electron

potential, the external gate and doping potentials, and the structural quantum-well potential profile. Note that the gap is $\Delta = \varepsilon_o - \varepsilon_e = 2\varepsilon_-$.

Theoretical approach. To calculate the edge spin density in the quasi-ballistic regime we follow the method developed in Refs. [20, 21] for the case of the single-subband Rashba Hamiltonian. Assuming that the spatial scale of the edge spin accumulation Λ is much smaller than the mean free path l , we solve the edge spin problem by the method of scattering states, i.e., we find the exact quantum mechanical solution of the electron scattering by an impenetrable straight boundary [Fig. 1(a)] at a given Fermi energy. These solutions are then used in the calculation of the (mean) spin density profile. The populations of the incoming states are found from the solution of the kinetic equation for the spin-density matrix in the bulk (2D) of the sample in the presence of electric field, see SM.

The Hamiltonian (2) has 4 eigensolutions $\Psi_{i,s}$, $\Psi_{1,\uparrow}$, $\Psi_{1,\downarrow}$, $\Psi_{2,\uparrow}$, $\Psi_{2,\downarrow}$ (see SM for their explicit form) with the corresponding energy spectrum

$$\varepsilon_{1,2}(p) = \frac{p^2}{2m} + \varepsilon_\pm \mp \sqrt{\varepsilon_\pm^2 + \eta^2 p^2 / \hbar^2}, \quad (3)$$

where the subscript $i = 1, 2$ corresponds to the lower (higher) in energy sub-band. Each sub-band is doubly degenerate with respect to the "spin direction" $s = \uparrow, \downarrow$ (Kramers pairs). Upon scattering by the straight boundary where energy and momentum p_y along the boundary are conserved, the states in the pair $\Psi_{1,\uparrow}(\varphi_1, \theta_1), \Psi_{2,\downarrow}(\varphi_2, \theta_2)$ mix up and form two scattering states, Eqs. (4),(5) [similarly for the pair $\Psi_{1,\downarrow}(\varphi_1, \theta_1), \Psi_{2,\uparrow}(\varphi_2, \theta_2)$]. For this pair of scattering states, we have the following boundary condition for the scattering by a hard wall located at $x = 0$ [Fig. 1(a)]

$$\tilde{\Psi}_{1,\uparrow}(x, y)|_{x=0} = e^{ik_y y} [\Psi_{1,\uparrow}(\pi - \varphi_1, \theta_1) e^{-ik_1 x} + F_{1,\uparrow}^{1,\uparrow} \Psi_{1,\uparrow}(\varphi_1, \theta_1) e^{ik_1 x} + F_{1,\uparrow}^{2,\downarrow} \Psi_{2,\downarrow}(\varphi_2, \theta_2) e^{ik_2 x}]|_{x=0} = 0, \quad (4)$$

$$\tilde{\Psi}_{2,\downarrow}(x, y)|_{x=0} = e^{ik_y y} [\Psi_{2,\downarrow}(\pi - \varphi_2, \theta_2) e^{-ik_2 x} + F_{2,\downarrow}^{1,\uparrow} \Psi_{1,\uparrow}(\varphi_1, \theta_1) e^{ik_1 x} + F_{2,\downarrow}^{2,\downarrow} \Psi_{2,\downarrow}(\varphi_2, \theta_2) e^{ik_2 x}]|_{x=0} = 0, \quad (5)$$

with $p_1^2 = \hbar^2(k_y^2 + k_1^2)$, $p_2^2 = \hbar^2(k_y^2 + k_2^2)$, $\varepsilon_1(p_1) = \varepsilon_2(p_2) = \varepsilon$. The momenta p_1, p_2 describe states belonging to subbands 1 and 2 for a given energy ε , see Fig. 1(b). The angles φ_1, φ_2 (between the corresponding momenta and the positive direction of the x -axis) are expressed as $\sin(\varphi_1) = \hbar k_y / p_1$ and $\sin(\varphi_2) = \hbar k_y / p_2$. The angles θ_1, θ_2 are defined via $\cos \theta_{1,2} = 1 / \sqrt{1 + (2\eta p_{1,2} / \hbar \Delta)^2}$. The expressions for the scattering amplitudes ($F_{1,\uparrow}^{1,\uparrow}$, etc.) and the corresponding components of the unitary scattering matrix \hat{S} are presented in SM. Similar equations can be written for the pair $\Psi_{1,\downarrow}(\varphi_1), \Psi_{2,\uparrow}(\varphi_2)$, and the corresponding scattering matrix elements are also determined.

The expectation value of the z component of the spin as a function of coordinates is given by the following expression:

$$\langle S_z(x) \rangle = \sum_{i,s} \int \frac{dk_y}{(2\pi)^2} \frac{d\varepsilon}{v_{x,i}} f_i(\varepsilon, k_y) \times \langle \tilde{\Psi}_{i,s}(x) | \hat{S}_z | \tilde{\Psi}_{i,s}(x) \rangle \quad (6)$$

Here $f_i(\varepsilon, k_y)$ is the distribution function of the electron state in the sub-band i for a given energy and given wave vector k_y along the boundary and the group velocity is $v_{x,i} = \partial \varepsilon_i / \partial p_x$.

We can then calculate the most important part of the edge spin density which is smooth on the scale of the

Fermi wave length [31] and involves the interference of the outgoing waves [two last terms in Eqs. (4) and (5)]. The corresponding formula for $\langle S_z(x) \rangle$ valid for general values of the parameters (in the case when both subbands are occupied) is presented in the SM. In the most important case $p_1 - p_2 \ll p_F$, when the energy separation between two sub-bands $\sqrt{\Delta^2 + 4\eta^2 k_F^2}$ is much smaller than the Fermi energy, the edge spin density for arbitrary values of the parameter $\xi = L_\Delta/L_s$ reads

$$\langle S_z(x) \rangle = -\sin^2 \theta \int \frac{dk_y k_y}{(2\pi)^2} \frac{d\varepsilon}{\varepsilon_F} \sin\left(\frac{x}{\Lambda \sqrt{1 - (k_y/k_F)^2}}\right) \times [f_1(\varepsilon, k_y) - f_2(\varepsilon, k_y)].$$

Here $\varepsilon_F = p_F^2/2m$ is the Fermi energy. While deriving Eq. (7), we used that $\theta_1 - \theta_2 \ll \theta_{1,2}$, and $\varphi_2 - \varphi_1 \ll \varphi_{1,2}$. The difference of the distribution functions entering Eq. (7) is calculated in the SM assuming the set of inequalities $k_F^{-1} \ll d \ll L_s$, where d is the correlation radius of the impurity potential in the bulk of the structure. The first condition means that the scattering in the bulk is of the small-angle type. Both conditions are fulfilled for a high mobility GaAs structure. The final result derived from Eq. (7) reads

$$\langle S_z(x) \rangle = \frac{3k_E}{L_s} \Phi(\xi) J(x/\Lambda); \quad \Phi(\xi) = \frac{\xi}{(2\xi^2 + 1)\sqrt{\xi^2 + 1}}. \quad (8)$$

with the spatial dependence given by the integral

$$J\left(\frac{x}{\Lambda}\right) = \int_0^1 \frac{dz z^2}{\pi^2} \sin\left(\frac{x}{\Lambda \sqrt{1 - z^2}}\right), \quad \Lambda = \frac{L_\Delta L_s}{\sqrt{L_\Delta^2 + L_s^2}}. \quad (9)$$

We recall that Λ is the characteristic spatial scale of the edge spin density. For $x \ll \Lambda$ we have $J(x) \propto x/\Lambda$. In the opposite limit $x \gg \Lambda$, we obtain $J(x) \propto (\Lambda/x)^{3/2} \cos[(x/\Lambda) + \pi/4]$.

Weak SO coupling: $L_s \gg L_\Delta$. To contrast our results with the usual one-band Rashba case it is instructive to consider here the limit of a weak SO coupling $2\eta k_F \ll \Delta$. In this limit we can calculate the difference of the distribution functions entering Eq. (7) using their standard expressions at $\eta = 0$ (see also SM), i.e.,

$$f_{1,2} = (eE\hbar k_y/m)\tau_{tr}(p_{1,2})\partial f_0/\partial\varepsilon, \quad (10)$$

where f_0 is the Fermi function, the electric field E is directed along the y -axis, and $\tau_{tr}(p)$ is the momentum-dependent transport scattering time calculated within the Born approximation due to impurity scattering in the bulk. The values of p_1, p_2 are related through $\varepsilon_1(p_1) = \varepsilon_2(p_2) = \varepsilon = \varepsilon_F$, Fig. 1(b). Using the condition $k_F d \gg 1$ (small-angle scattering in bulk), we obtain $(\tau_{tr}(p_1) - \tau_{tr}(p_2))/\tau_{tr} \approx 3(p_1 - p_2)/p_F \approx (3/(k_F L_\Delta))$. [32] We note that compared to the usual Rashba one-band case the difference of the distribution functions considered here is finite at $\eta = 0$, and is of the first order in

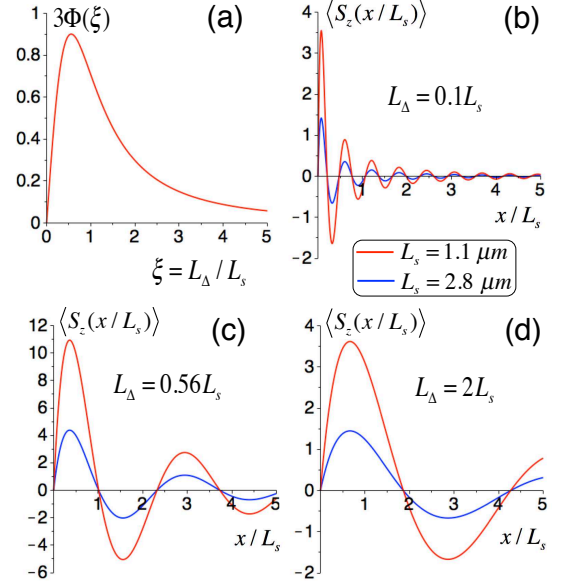


Figure 2. $\Phi(\xi)$ vs. ξ a) and the edge spin density $\langle S_z(x) \rangle$ in units of 10^6 cm^{-2} for distinct ratios L_Δ/L_s and two different values of L_s b)-d), as a function of x/L_s . Note that $\Phi(\xi)$ has a maximum at $\xi \sim 0.56 = L_\Delta/L_s$. The amplitude of the oscillations is reduced as L_s increase (cf. blue and red curves in b)-d).)

$p_1 - p_2 = \hbar/L_\Delta$. Since the SO coupling is weak, the probability of the spin flip is small which shows up as the small factor $\sin^2 \theta \approx L_\Delta^2/L_s^2 \ll 1$ in Eq. (7), and finally we obtain

$$\langle S_z(x) \rangle = 3k_E \frac{L_\Delta}{L_s^2} J(x/\Lambda), \quad (11)$$

which coincides with the result which follows from Eq.(8) in the limit $\xi \rightarrow 0$.

The calculated edge spin density Eq. (8) is maximal at $L_\Delta \approx L_s$ when it is of the order of k_E/L_s . With decreasing the gap ($L_s < L_\Delta$) the spectrum approaches the usual Rashba model type (doubly degenerate), and because of the specific cancellation inherent in that model $\langle S_z(x) \rangle$ decreases in magnitude as $k_E L_s/L_\Delta^2$ [see Fig. 2(a)], finally approaching the limit calculated in Ref. 21 given by $\simeq (k_E/L_s)(d^2/L_s^2)$ [see also Eq. (1)]. Thus for a given strength of the SO interaction, the magnitude of the edge spin density has non-monotonic dependence as a function of the L_Δ (or Δ), Fig. 2(a). We note that if one takes for the ratio $d/L_s = 0.1$, then the edge spin density obtained in Ref. [21] for the usual Rashba system with one sub-band equals in magnitude the density which follows from Eq. (8) at $\xi \approx 35$, where the latter is three orders of magnitude smaller than its maximal value at $\xi = 0.56$.

Comparison with the experiment. The experimental estimate of L_Δ is $\approx 1.4 \times 10^{-5} \text{ cm}$. For L_s we take two

characteristic lengths $1.1\mu\text{m}$ and $2.8\mu\text{m}$. Note that the corresponding values of η are consistent with the ones obtained from the theoretical calculations [33] for structures similar to that used in the experiment of Ref. [22]. Thus the value $\xi = 0.1$ will reasonably correspond the above chosen lengths. Calculating τ_{tr} from the mobility $1.9 \times 10^6 \text{cm}^2/\text{Vs}$, and using $E = 0.05 \text{mV}/\mu\text{m}$ for the electric field in the quasi-ballistic region of the sample (both the mobility and E are taken from Ref. [22]), we plot $\langle S_z(x) \rangle$, see Fig. 2(b). The exact experimental value of the edge spin density is not known; the authors of Ref. [22] have estimated the threshold minimal value compatible with their observation as $3 \times 10^6 \text{cm}^{-2}$. Hence this number is consistent with our calculation. In addition, we stress that the procedure just described, i.e., comparison of our theoretical predictions for the edge spin density with the experimental value of this quantity, allows one to extract the value of η .

In conclusion, using a Rashba-like SO interaction arising from the coupling between two sub-band states of opposite parities in a symmetric two-subband quantum well, we have explained the great difference between the edge spin density in a bilayer structure as compared to the one in a single-layer configuration observed in the experiment of Ref. [22]. The presence of the gap between the two sub-bands governs the effective strength of the inter-subband SO interaction and changes drastically the picture of the edge spin accumulation. Thus by varying the gap value one can easily proceed from the regime of strong spin accumulation to the regime of weak spin accumulation. This opens up the possibility for the design of new spintronic devices.

We acknowledge financial support from FAPESP (Fundação de Apoio à Pesquisa do Estado de São Paulo). Helpful discussions with G. Gusev and F. G. G. Hernandez are greatly appreciated. A. Khaetskii is also grateful to Instituto de Física de São Carlos of the University of São Paulo for the hospitality.

[1] H.A. Engel, E.I. Rashba, and B.I. Halperin, in Handbook of Magnetism and Advanced Magnetic Materials, ed. by H. Kronmuller and S. Parkin, Vol.5 (John Wiley and Sons, New York, 2007).

[2] M.I. Dyakonov, and A.V. Khaetskii, "Spin Hall effect", in Spin Physics in Semiconductors, ed. by M.I. Dyakonov (Springer, Berlin, 2008).

[3] I. Zutíć, J. Fabian, and S. Das Sarma, Rev. Mod. Phys. **76**, 323 (2004).

[4] M.I. Dyakonov and V. I. Perel, JETP Lett. **13**, 467 (1971).

[5] J.E. Hirsch, Phys. Rev. Lett. **83**, 1834 (1999).

[6] M.I. Dyakonov, and A.V. Khaetskii, Sov. Phys. JETP **59**, 1072 (1984).

[7] A.V. Khaetskii, Sov. Phys. Semicond. **18**, 1091 (1984).

[8] S. Murakami, N. Nagaosa, S.-C. Zhang, Science **301**,

1348 (2003).

[9] J. Sinova, D. Culcer, Q. Niu, N.A. Sinitsyn, T. Jungwirth, A.H. MacDonald, Phys. Rev. Lett. **92**, 126603 (2004).

[10] Y. K. Kato, R. C. Myers, A. C. Gossard, and D. D. Awschalom, Science **306**, 1910 (2004).

[11] J. Wunderlich, B. Kaestner, J. Sinova, and T. Jungwirth, Phys. Rev. Lett. **94**, 047204 (2005).

[12] K. Nomura, J. Wunderlich, J. Sinova, B. Kaestner, A. H. MacDonald, and T. Jungwirth, Phys. Rev. B **72**, 245330 (2005).

[13] Y. Tserkovnyak, B. I. Halperin, A. A. Kovalev, and A. Brataas, Phys. Rev. B **76**, 085319 (2007).

[14] O. Bleibaum, Phys. Rev. B **74**, 113309 (2006).

[15] I. Adagideli and G. E.W. Bauer, Phys. Rev. Lett. **95**, 256602 (2005).

[16] B. K. Nikolić, S. Souma, L. P. Zarbo, and J. Sinova, Phys. Rev. Lett. **95**, 046601 (2005).

[17] G. Usaj and C. A. Balseiro, Europhys. Lett. **72**, 631 (2005).

[18] V. A. Zyuzin, P. G. Silvestrov, and E. G. Mishchenko, Phys. Rev. Lett. **99**, 106601 (2007).

[19] P. G. Silvestrov, V. A. Zyuzin, and E. G. Mishchenko, Phys. Rev. Lett. **102**, 196802 (2009).

[20] A. Khaetskii and E. Sukhorukov, Phys. Rev. B **87**, 075303 (2013).

[21] A. Khaetskii, Phys. Rev. B **89**, 195408 (2014).

[22] F. G. G. Hernandez, L. M. Nunes, G. M. Gusev, and A. K. Bakarov, Phys. Rev. B **88**, 161305(R) (2013).

[23] One-subband or two-subband configurations were realized experimentally using symmetric quantum wells of different widths. A 14 nm wide sample contained only one subband but a 45 nm wide sample contained two (even and odd) subbands. Due to the Coulomb repulsion of the electrons in the wide quantum well, the charge distribution resulted in a bilayer electron system with a soft barrier inside the well. Tunneling through this barrier leads to the symmetric-antisymmetric splitting Δ_{SAS} for which we use the notation Δ .

[24] F. T. Vasko, JETP Letters **30**, 541 (1979); Yu. Bychkov and E. I. Rashba, JETP Letters **39**, 78 (1984).

[25] M. I. Dyakonov and V. Kachorovskii, Sov. Phys. Semicond. **20**, 110 (1986).

[26] E. Bernardes, J. Schliemann, M. Lee, J. C. Egues, and D. Loss, Phys. Rev. Lett. **99**, 076603 (2007).

[27] R. S. Calsaverini, E. S. Bernardes, J. C. Egues, and D. Loss, Phys. Rev. B **78**, 155313 (2008).

[28] A. Khaetskii, Phys. Rev. B **73**, 115323 (2006).

[29] A.V. Shytov, E.G.Mishchenko, H.-A. Engel, and B. I. Halperin, Phys. Rev. B **73**, 075316 (2006).

[30] For the two-subband wide-well sample of Ref. [22] the total electron density $n = 9.2 \times 10^{11} \text{cm}^{-2}$ and the Fermi wave vectors $k_{F,1} = k_{F,2} = k_F = \sqrt{2\pi n/2} = 1.7 \times 10^6 \text{cm}^{-1}$. The Fermi energy is $\varepsilon_F = \hbar^2 k_F^2 / 2m = 16.4 \text{meV}$ (assuming $m = 0.067m_0$ for a GaAs well). Note that $\varepsilon_F \gg \Delta = 1.4 \text{meV}$ in Ref. [22].

[31] A fast contribution to the edge spin density which oscillates as function of x with $2k_F$ wave vector, gives parametrically smaller contribution to the total spin $\int_0^\infty dx \langle S_z(x) \rangle$, and we omit it. [21]

[32] We consider a high mobility 2D structure, where scattering is due to the long-range disorder caused by the donor layer located at distance d from the 2D gas. Since $k_F d \gg 1$, the characteristic scattering angle is

$\simeq 1/k_F d \ll 1$. Therefore the *transport* scattering time calculated in the Born approximation at a given momentum p is $\tau_{tr}(p) = Ap^3$, where A is some constant, see SM.

[33] Jiyong Fu and J. Carlos Egues, Phys. Rev. B **91**, 075408 (2015).